On a boundary condition used in Virtual Fields methods

S. J. Subramanian[1], Nigamaa Nayakanti

Department of Engineering Design, Indian Institute of Technology Madras, Chennai, India 600036

Abstract

The Virtual Fields Method (VFM) and the Eigenfunction Virtual Fields Method (EVFM) are inverse techniques for estimating constitutive properties from full-field experimental data. In these, a set of virtual fields are used in the Principle of Virtual Work (PVW) to yield a system of algebraic equations for the unknown material parameters. In a typical experiment, one does not know the distribution of tractions over the external surface of the specimen, but the total force is generally measured. In order to still enable evaluation of the external virtual work integral that appears in PVW, the virtual displacements are commonly restricted to be uniform over the portion of the exterior surface where tractions are prescribed so that the external virtual work is simply the inner product of the known total force vector and the uniform value of the chosen virtual displacement vector. In this work, we show that this constraint is unnecessary, and its removal leads to a more flexible version of EVFM. The proposed modification is used to obtain orthotropic elastic constants from an unnotched Iosipescu test, and is shown to yield tighter estimates than previously obtained wherein the boundary

[1] *email*: shankar_sj@iitm.ac.in

virtual displacements were constrained to be uniform. The removal of the constraint also results in a more flexible EVFM formulation capable of dealing with material heterogeneity, missing data and discontinuities in specimen geometry.

Keywords: Virtual Field Method; Eigenfunction Virtual Fields Method; orthotropic elasticity; full-field measurement; Principal Component Analysis; eigenfunction; inverse problem; noise

---

1. Introduction

The Virtual Fields Method (VFM - Grediac, 1989; Pierron and Grediac, 2012) is a versatile technique for obtaining constitutive parameters from full-field kinematic measurements. Several refinements of VFM have been proposed over the years, using piece-wise continuous virtual fields (VFs) as well as ones continuous over the entire domain of interest. VFM has been successfully applied to the evaluation of parameters describing a number of constitutive models (Pierron and Grediac, 2012). Recently, a novel variant of VFM, called the Eigenfunction Virtual Fields Method (EVFM) has been proposed (Subramanian, 2013; Nayakanti and Subramanian, 2013), wherein VFs are systematically constructed using the eigenfunctions (Grama and Subramanian, 2013) of the measured strain fields. The VFs so chosen have clear physical meaning and are directly determined using Principal Component Analysis of the measured strains.

VFM and EVFM are based on the Principle of Virtual Work (PVW -

Malvern, 1977), which may be stated as

$$\int_V \boldsymbol{\sigma} : \boldsymbol{\varepsilon}^* \mathrm{d}V = \int_{S_T} \boldsymbol{t} \cdot \boldsymbol{u}^* \mathrm{d}A, \tag{1}$$

where V is the volume occupied by the solid of interest, S_T is the portion of the exterior surface of the solid where tractions are prescribed, $\boldsymbol{\sigma}$ is any statically admissible stress field, $\boldsymbol{t}$ is the (true) traction vector specified on S_T, $\boldsymbol{u}^*$ is any kinematically admissible virtual displacement field and $\boldsymbol{\varepsilon}^* = \frac{1}{2}\left(\nabla \boldsymbol{u}^* + \nabla \boldsymbol{u}^{*T}\right)$ is the virtual strain field obtained by differentiating the virtual displacement field $\boldsymbol{u}^*$ with respect to the current configuration (Malvern, 1977). In the above expression, body forces and inertial forces have been assumed to be small enough to be ignored. The central idea in both VFM and EVFM is that by choosing different VFs in Eqn. (1), a system of algebraic equations can be generated and solved for the unknown material parameters. Piece-wise continuous or full-domain VFs are used in conventional VFM and the unknown polynomial coefficients are obtained through optimization with respect to measurement noise, whereas VFs based on eigenfunctions of measured strain fields are used in EVFM without the need to compute any additional parameters.

In Nayakanti and Subramanian (2013), EVFM was used to determine orthotropic elastic constants and the results compared to those obtained using conventional VFM. Linear equations were generated using two sub-domains in the plane-stress Iosipescu specimen: sub-domain A from the middle of the specimen spanning the entire height and sub-domain B spanning the entire length of the specimen (Fig. 1). Thirty realizations of Gaussian noise of fixed variance were added to strain fields generated using FEM and the

resulting noisy strain fields used to compute the elastic constants. It was observed that while EVFM produced good estimates for low to moderate noise, at high levels of noise, coefficients of variation (CVs) for two of the elastic parameters were worse than those obtained using conventional VFM. Nayakanti and Subramanian (2013) traced the high CVs to the pronounced noise in the third eigenvector of the column-augmented strain matrix of sub-domain B that was used to generate one of the four linear equations. The other three equations, which were all generated using the first eigenvector are more robust and are much less affected by the noise in the strain data.

In the present work, we present an improvement to the EVFM approach described in Nayakanti and Subramanian (2013), wherein the virtual displacement field was chosen to be uniform over the regions over which tractions were prescribed. This constraint on the VFs is inherited from conventional VFM and it enables simple computation of the external virtual work over the part of the external surface where only the total loads are known and not the actual distribution of tractions. For the unnotched Iosipescu test specimen studied in Nayakanti and Subramanian (2013), this constraint implies that the first left eigenfunction of the column-augmented strain field of sub-domain A cannot be used to generate a virtual field since it produces virtual displacements that vary over the area on which external tractions are applied. In this work, we show that this constraint is unnecessary and its removal leads to a versatile version of EVFM. Indeed, this boundary condition may be removed from conventional VFM as well.

The rest of the paper is organized as follows. In section 2, we describe the boundary condition under consideration and the work performed

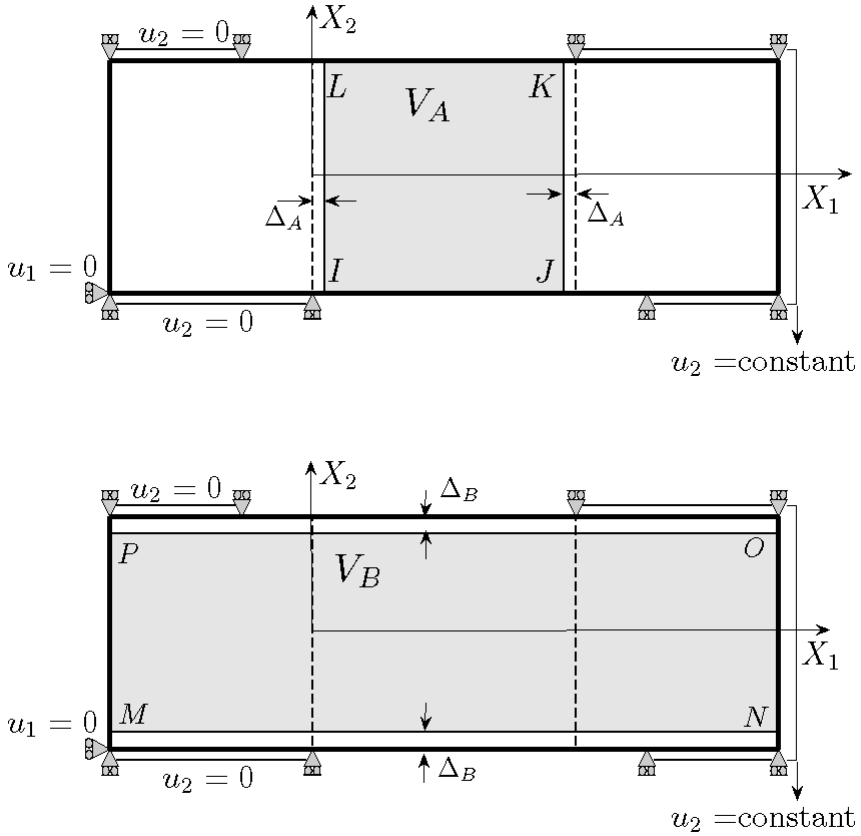

Figure 1: Sub-domains A (shaded region, top) and B (shaded region, bottom) of the unnotched Iosipescu specimen used by Nayakanti and Subramanian (2013) to generate EVFM equations. Δ_A and Δ_B are thin strips excluded from the sub-domains so that they are free of any prescribed displacements.

in Nayakanti and Subramanian (2013), and present two new virtual fields that replace the third and fourth equations used therein. It is worth noting that these new virtual fields are also based on the first eigenfunction, just as the first two virtual fields are, and therefore lead to a robust system of equations in the unknown material parameters. In section 3, the modified EVFM equations are developed and in section 4, the results of using these new equations to evaluate the same material parameters estimated in Nayakanti and Subramanian (2013) are presented and discussed. The main conclusions of the present work are summarized in Section 5.

2. Boundary conditions in the Virtual Fields Methods

In conventional VFM as well as EVFM work to date, the external virtual work term (r.h.s. of Eqn. 1) is computed by assuming uniform virtual displacement fields so that the work is simply the inner product of the total force vector and the chosen virtual displacement vector. This condition has been enforced for both full-domain as well as piece-wise VF in conventional VFM (Grediac et al., 2002; Pierron and Grediac, 2012) as well as in EVFM (Nayakanti and Subramanian, 2013).

In this work, we investigate this condition in detail. We begin by observing that although the point-wise traction vector is not known on S_T, it follows from the definition of the traction vector and the elastic constitutive equations that

$$\boldsymbol{t} = \boldsymbol{\sigma}\boldsymbol{n} = \boldsymbol{C}\boldsymbol{\varepsilon}\boldsymbol{n}, \tag{2}$$

where $\boldsymbol{C}$ is the elasticity tensor, and $\boldsymbol{n}$ is the exterior unit normal to S_T at the point of interest. The tractions that appear in the external virtual work

integral are now linear combinations of the elastic constants, from which it follows that the external virtual work may also be expressed as a linear combination of the elastic constants. Likewise, the stress appearing in the internal virtual work expression in Eqn. 1 is also known in terms of the elastic constants, from which it is evident that the internal virtual work may also be expressed as a linear combination of the elastic constants. Thus, any virtual field that varies along S_T is seen to yield a homogeneous equation in the unknown material parameters. If there are n elastic constants to be determined, one is free to choose $(n-1)$ virtual fields that vary arbitrarily over S_T to generate $(n-1)$ homogeneous equations, from which $n-1$ ratios between the n constants may be obtained. In order to obtain exact numerical values for the constants, only one additional inhomogeneous algebraic equation is required and this may be straightforwardly obtained using the conventional constrained virtual displacement field.

We adopt this new approach to choosing virtual fields for the unnotched Iosipescu specimen (Fig. 1) considered in Nayakanti and Subramanian (2013). The resulting EVFM equations are listed in the next section.

3. Modified EVFM equations

The unnotched Iosipescu test is well researched in the literature; Pierron and Grediac (2012) present several case studies based on this geometry and Nayakanti and Subramanian (2013) use EVFM to obtain estimates of orthotropic elastic constants. Of the four VF used by Nayakanti and Sub-

ramanian (2013), two are based on the *first right eigenfunction* $\boldsymbol{r}_1$ [2] of the row-augmented strain matrix $\boldsymbol{E}^r$ of sub-domain A, the third is based on the *first left eigenfunction* $\boldsymbol{l}_1$ of the column-augmented strain matrix $\boldsymbol{E}^c$ of sub-domain B and the last is based on the *third left eigenfunction* $\boldsymbol{l}_3$ of the column-augmented strain matrix $\boldsymbol{E}^c$ of sub-domain B. The elastic constants are shown to be good for low to moderate noise levels in the input strain matrices, but for noise amplitude of 0.001, the coefficients of variation of two of the constants is seen to be excessively high compared to those obtained using conventional VFM.

The large coefficients of variation were traced back to the linear equation obtained using the third eigenvector. In fact, one of the two coefficients in this equation shows a coefficient of variation that is two orders of magnitude larger than that of any of the other coefficients. The reason for this coefficient of variation being high is also easily understood; it is obtained from an inner product of the strain component ε_1 with the third left eigenvector of the column-augmented matrix $\boldsymbol{E}^c$. Since ε_1 has the smallest average magnitude over the domain considered and the third left eigenvector of $\boldsymbol{E}^c$ is much more susceptible to noise, the resulting coefficient has a high CV.

If instead of using the third eigenvector, we were to generate another equation using the first eigenvector, then the resulting equations may be

[2] We introduce the following modification to the notation introduced in Subramanian (2013): we reserve $\boldsymbol{r}$ for the right eigenfunction of $\boldsymbol{E}^r$, without carrying the superscript r. Similarly, $\boldsymbol{l}$ denotes the left eigenfunction of $\boldsymbol{E}^c$. These simplifications introduce no ambiguity since the left eigenfunctions of $\boldsymbol{E}^r$ and right eigenfunctions of $\boldsymbol{E}^c$ are not used in the present EVFM formulation. Further, we use the subscript to denote eigenfunction number, so that $\boldsymbol{r}_i$ and $\boldsymbol{l}_j$ stand respectively for the ith right eigenfunction of $\boldsymbol{E}^r$ and jth left eigenfunction of $\boldsymbol{E}^c$.

expected to be more robust to noise. However, when the virtual displacement is constrained to be uniform along S_T, one cannot generate another virtual field using the first left or right eigenvector. In the light of the relaxation of this constraint as explained in the previous section, we are free to generate all four equations using the first left and right eigenvectors as follows. With the use of unconstrained virtual fields, it is no longer necessary to use the two sub-domains A and B, as done in (Nayakanti and Subramanian, 2013) and we use only sub-domain A in the present work (Figs. 1). Since the average strain magnitude is higher in sub-domain A than in sub-domain B, one can expect the effect of noise to be lower if sub-domain A is used. The horizontal edges IJ and KL of sub-domain A are free of tractions, while equilibrium dictates that the resultant vertical force is equal to the applied load F on the edges JK and IL (Fig. 2).

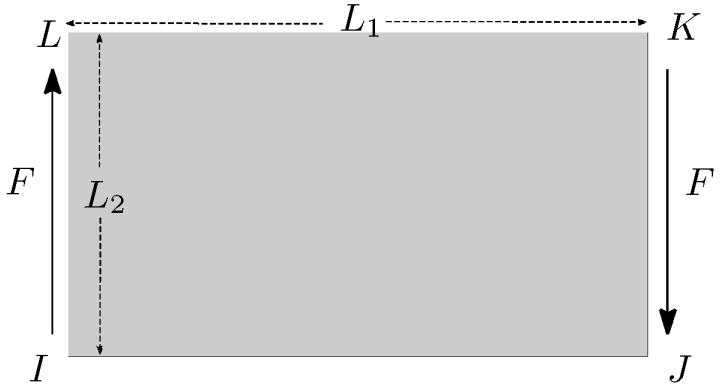

Figure 2: Force resultant along the 2-direction on the exterior surfaces of sub-domain A

As in Nayakanti and Subramanian (2013), we employ piece-wise continuous versions of the eigenfunctions and their integrals to compute virtual work. Denoting by ΔX_1 and ΔX_2 the grid sizes along the X_1 and X_2 directions, $(X_1)^k$ and $(X_2)^k$ the X_1 and X_2 values at the kth grid location, and

r_k and l_k the kth component of a generic right and left eigenfunctions $\boldsymbol{r}$ and $\boldsymbol{l}$ respectively, these are defined as

$$f_n(X_1;\boldsymbol{r}) = \sum_{k=1}^{n} N_k(X_1)\ r_k; \quad N_k(X_1) = \begin{cases} 1, \text{ if } (X_1)^k - \frac{\Delta X_1}{2} < X_1 < (X_1)^k + \frac{\Delta X_1}{2} \\ 0, \text{ otherwise} \end{cases}, \tag{3}$$

$$f_m(X_2;\boldsymbol{l}) = \sum_{k=1}^{m} N_k(X_2)\ l_k; \quad N_k(X_2) = \begin{cases} 1, \text{ if } (X_2)^k - \frac{\Delta X_2}{2} < X_2 < (X_2)^k + \frac{\Delta X_2}{2} \\ 0, \text{ otherwise} \end{cases}. \tag{4}$$

The integrals of these piecewise-constant functions, which are used in the evaluation of the virtual work integrals, are defined as

$$P_n(X_1;\boldsymbol{r}) = \int_0^{X_1} f_n(s;\boldsymbol{r})\mathrm{d}s; \quad P_m(X_2;\boldsymbol{l}) = \int_0^{X_2} f_m(s;\boldsymbol{l})\mathrm{d}s \tag{5}$$

Since the left and right eigenfunctions are obtained through SVD, they are orthogonal (Strang, 2006), and therefore, so are their piece-wise continuous versions f_m and f_n. Thus, for the ith and jth left and right eigenfunctions, one obtains (Subramanian, 2013)

$$\begin{aligned} \int_0^{L_1} f_n(X_1;\boldsymbol{r}_i) f_n(X_1;\boldsymbol{r}_j)\mathrm{d}X_1 &= \delta_{ij}\Delta X_1 \\ \int_0^{L_2} f_m(X_2;\boldsymbol{l}_i) f_m(X_2;\boldsymbol{l}_j)\mathrm{d}X_2 &= \delta_{ij}\Delta X_2 \end{aligned} \tag{6}$$

where δ_{ij} is the Kronecker delta, equal to 1 if $i = j$ and 0 otherwise.

The strain component fields ε_1, ε_2 and ε_6 are expressed as linear combinations of the piecewise-continuous p dominant (Grama and Subramanian,

2013)

- right eigenfunctions

$$\begin{aligned}
\varepsilon_1(X_1,(X_2)^k) &= \sum_{t=1}^{p}(\widetilde{\mathbf{A}}_1^r)^{(k,t)} f_n(X_1;\boldsymbol{r}_t)\\
\varepsilon_2(X_1,(X_2)^k) &= \sum_{t=1}^{p}(\widetilde{\mathbf{A}}_2^r)^{(k,t)} f_n(X_1;\boldsymbol{r}_t)\\
\varepsilon_6(X_1,(X_2)^k) &= \sum_{t=1}^{p}(\widetilde{\mathbf{A}}_6^r)^{(k,t)} f_n(X_1;\boldsymbol{r}_t)
\end{aligned} \tag{7}$$

- or left eigenfunctions:

$$\begin{aligned}
\varepsilon_1((X_1)^k,X_2) &= \sum_{t=1}^{p}(\widetilde{\mathbf{A}}_1^c)^{(t,k)} f_m(X_2;\boldsymbol{l}_t)\\
\varepsilon_2((X_1)^k,X_2) &= \sum_{t=1}^{p}(\widetilde{\mathbf{A}}_2^c)^{(t,k)} f_m(X_2;\boldsymbol{l}_t)\\
\varepsilon_6((X_1)^k,X_2) &= \sum_{t=1}^{p}(\widetilde{\mathbf{A}}_6^c)^{(t,k)} f_m(X_2;\boldsymbol{l}_t)
\end{aligned} \tag{8}$$

The $\widetilde{\mathbf{A}}$ matrices are obtained through products of the strain matrices with the eigenvectors, as explained in Subramanian (2013).

In the present work, the first two virtual fields remain unchanged from those reported in Nayakanti and Subramanian (2013) and are based on $\boldsymbol{r}_1$, the first right eigenfunction of the row-augmented matrix $\boldsymbol{E}^r$:

166 • Virtual Field 1 (VF1):

$$\begin{aligned} u_1^* = 0; \quad u_2^* = P_n(X_1; \boldsymbol{r}_1) \\ \varepsilon_1^* = 0; \quad \varepsilon_2^* = 0; \quad \varepsilon_6^* = f_n(X_1; \boldsymbol{r}_1), \end{aligned} \tag{9}$$

167 • Virtual Field 2 (VF2):

$$\begin{aligned} u_1^* = P_n(X_1; \boldsymbol{r}_1); \quad u_2^* = 0 \\ \varepsilon_1^* = f_n(X_1; \boldsymbol{r}_1); \quad \varepsilon_2^* = 0; \quad \varepsilon_6^* = 0; \end{aligned} \tag{10}$$

168 VF1 represents a simple shear deformation while VF2 represents a non-
169 uniform elongation along the X_1 direction. Unlike in Nayakanti and Sub-
170 ramanian (2013), the third and fourth eigenfunctions are also generated in
171 the present work from sub-domain A and use $\boldsymbol{l}_1$, the first left eigenfunction
172 of the column-augmented matrix $\boldsymbol{E}^c$. VF3 also represents a simple shear de-
173 formation, while VF4 represents an elongation along the X_2 direction. These
174 eigenfunctions are expressed as:

175 • Virtual Field 3 (VF3):

$$\begin{aligned} u_1^* = P_m(X_2; \boldsymbol{l}_1); \quad u_2^* = 0; \\ \varepsilon_1^* = 0; \quad \varepsilon_2^* = 0; \quad \varepsilon_6^* = f_m(X_2, \boldsymbol{l}_1) \end{aligned} \tag{11}$$

176 • Virtual Field 4 (VF4):

$$\begin{aligned} u_1^* = 0; \quad u_2^* = P_m(X_2; \boldsymbol{l}_1) \\ \varepsilon_1^* = 0; \quad \varepsilon_2^* = f_m(X_2, \boldsymbol{l}_1); \quad \varepsilon_6^* = 0 \end{aligned} \tag{12}$$

When VF1 and VF2 are substituted into Eqn. (1), the resulting equations are the same as those of Nayakanti and Subramanian (2013). Substitution of VF3 and VF4 into Eqn. (1) yields respectively

$$\int_V (Q_{66}\varepsilon_6) f_m(X_2;\boldsymbol{l}_1)\mathrm{d}V = h\int_0^{L_2} \left[\sigma_1(L_1,X_2) - \sigma_1(0,X_2)\right] P_m(X_2;\boldsymbol{l}_1)\mathrm{d}X_2$$

177

$$= h\int_0^{L_2} \left[(Q_{11}\varepsilon_1(L_1,X_2) + Q_{12}\varepsilon_2(L_1,X_2)) - (Q_{11}\varepsilon_1(0,X_2) + Q_{12}\varepsilon_2(0,X_2))\right] P_m(X_2;\boldsymbol{l}_1)\mathrm{d}X_2 \tag{13}$$

$$\int_V (Q_{12}\varepsilon_1 + Q_{22}\varepsilon_2)\, f_m(X_2;\boldsymbol{l}_1)\mathrm{d}V = h\int_0^{L_2} \left[\sigma_6(L_1,X_2) - \sigma_6(0,X_2)\right] P_m(X_2;\boldsymbol{l}_1)\mathrm{d}X_2$$

178

$$= Q_{66}\int_0^{L_2} \left[\varepsilon_6(L_1,X_2) - \varepsilon_6(0,X_2))\right] P_m(X_2;\boldsymbol{l}_1)\mathrm{d}X_2 \tag{14}$$

179 Simplifying these expressions by first expanding the strains in terms of
180 the left eigenfunctions (Eqn. 8) and then using orthogonality of the eigen-
181 functions, we obtain two linear equations in the unknowns (Appendix A),
182 which together with those from VF1 and VF2 may be written as:

$$\begin{bmatrix} 0 & 0 & 0 & P_{14} \\ P_{21} & 0 & P_{23} & 0 \\ P_{31} & 0 & P_{33} & P_{34} \\ 0 & P_{42} & P_{43} & P_{44} \end{bmatrix} \begin{Bmatrix} Q_{11} \\ Q_{22} \\ Q_{12} \\ Q_{66} \end{Bmatrix} = \begin{Bmatrix} R_1 \\ 0 \\ 0 \\ 0 \end{Bmatrix} \tag{15}$$

183 or more compactly in the form $\mathbf{PQ} = \mathbf{R}$. The elements of $\mathbf{P}$ and $\mathbf{R}$ are

found to be

$$
\begin{aligned}
P_{14} =& h\Delta X_2 \left[\sum_{k=1}^{m}(\widetilde{A_6^r})^{(k,1)}\right] \\
P_{21} =& \left[\sum_{k=1}^{m}(\widetilde{\mathbf{A}}_1^r)^{(k,1)}\right] \\
P_{23} =& \left[\sum_{k=1}^{m}(\widetilde{\mathbf{A}}_2^r)^{(k,1)}\right] \\
P_{31} =& \sum_{j=1}^{m}\left(\varepsilon_1^{(n,j)} - \varepsilon_1^{(1,j)}\right)\left\{\left[\sum_{k=1}^{j-1} l_1^k\right](\Delta X_2)^2 + \frac{l_1^j}{2}\left((X_2^{j+1})^2 - (X_2^j)^2\right) - l_1^j X_2^j \Delta X_2\right\} \\
P_{33} =& \sum_{j=1}^{m}\left(\varepsilon_2^{(n,j)} - \varepsilon_2^{(1,j)}\right)\left\{\left[\sum_{k=1}^{j-1} l_1^k\right](\Delta X_2)^2 + \frac{l_1^j}{2}\left((X_2^{j+1})^2 - (X_2^j)^2\right) - l_1^j X_2^j \Delta X_2\right\} \\
P_{34} =& -\Delta X_1 \Delta X_2 \sum_{k=1}^{n}(\widetilde{A_6^c})^{(1,k)} \\
P_{42} =& \Delta X_1 \Delta X_2 \sum_{k=1}^{n}(\widetilde{A_2^c})^{(1,k)} \\
P_{43} =& \Delta X_1 \Delta X_2 \sum_{k=1}^{n}(\widetilde{A_1^c})^{(1,k)} \\
P_{44} =& -\sum_{j=1}^{m}\left(\varepsilon_6^{(n,j)} - \varepsilon_6^{(1,j)}\right)\left\{\left[\sum_{k=1}^{j-1} l_1^k\right](\Delta X_2)^2 + \frac{l_1^j}{2}\left((X_2^{j+1})^2 - (X_2^j)^2\right) - l_1^j X_2^j \Delta X_2\right\} \\
R_1 =& F\sum_{t=1}^{n} r_1^t,
\end{aligned}
\tag{16}
$$

where $\varepsilon^{(n,j)}$ stands for the value of the strain component under consideration at the (n,j)th grid location and r_1^t and l_1^t refer to the tth component of $\boldsymbol{r}_1$ and $\boldsymbol{l}_1$ respectively.

4. Results and Discussion

The effect of noise on the estimated parameters was studied in Nayakanti and Subramanian (2013) by adding Gaussian noise of amplitude γ to the synthetic data generated using FEA. γ values up to 0.001 were studied and for each value, 30 realizations of noise were added to true strain data and the material properties computed. Here, we repeat this experiment for $\gamma = 0.001$, the most severe noise amplitude studied in Nayakanti and Subramanian (2013). For each of the 30 sets of noisy strain data, the entries of $\boldsymbol{P}$ and $\boldsymbol{R}$ (Eqn. 16) are computed and the system of equations Eqs. (15) solved for the parameters $Q11$, $Q12$, $Q22$ and $Q66$. For each material parameter, its mean value (μ_{ij}), standard deviation (s_{ij}) and coefficient of variation (CV $=s_{ij}/\mu_{ij}$) are computed. The mean values of all parameters are given in Table 1 and agree well with the true values. Evidently, the present approach yields unbiased estimators, although this claim must be verified through a more formal analysis of the bias and variance of the four estimators.

	Q_{11}	Q_{12}	Q_{22}	Q_{66}
True Value (GPa)	41.00	3.10	10.30	4.00
Present Method (GPa)	41.75	3.24	10.15	4.00

Table 1: Mean values of the 4 orthotropic elastic constants obtained using the present approach for a noise amplitude of 0.001.

The CVs of the parameters obtained using the present approach are summarized in Table 2, in which the comparison with the results of Pierron and Grediac (2012) and Nayakanti and Subramanian (2013) is also shown. Overall, the present work produces results that are better than those in Nayakanti and Subramanian (2013), especially for Q_{11} and Q_{12}, for which

Reference	$\frac{s_{11}}{\mu_{11}}$	$\frac{s_{12}}{\mu_{12}}$	$\frac{s_{22}}{\mu_{22}}$	$\frac{s_{66}}{\mu_{66}}$
Pierron and Grediac (2012), optimized polynomial	0.030	0.114	0.084	0.004
Pierron and Grediac (2012), piecewise polynomial	0.031	0.186	0.093	0.004
Nayakanti and Subramanian (2013)	0.751	0.741	0.014	0.001
Present Work	**0.083**	**0.115**	**0.026**	**0.001**

Table 2: CVs of the 4 orthotropic elastic constants obtained using the present approach and others in the literature for a noise amplitude of 0.001.

the CVs were greater than 0.7. The present results also compare favourably with both the optimized full-domain polynomial and piecewise polynomial approaches of Pierron and Grediac (2012).

The replacement of the noise-sensitive third eigenvector by the much more robust first eigenvector leads to estimates of the material properties that are on par with those obtained from conventional optimized VFM. The success of the present method also proves that the uniformity constraint on the virtual displacement fields is unnecessary and can be discarded for all but one of the equations.

The removal of this constraint has several significant implications for EVFM, and in fact, for conventional VFM too. With the constraint removed, it is no longer necessary to choose only those regions on whose boundaries the net force is known; one is now free to choose arbitrary domains that are entirely internal to the area of strain measurement. Such domains, as mentioned before, will yield homogeneous equations, which when coupled with one equation obtained from a domain on which an applied traction or a resultant is known, will suffice to yield unique numerical values for the material parameters. Freedom to choose an integration domain of arbitrary shape and size will enable study of material inhomogeneity at a scale hitherto

impossible with VF methods.

Moving the domain to interior regions also opens up the possibility of finding the best domain of all the possible domains available. Intuitively, the best domains will be those that offer the best signal-to-noise ratio. Thus, it might be possible to improve the present results further by optimizing choice of domains. Conversely, one can view the present results as being made more noise-sensitive by the inclusion of regions with poor signal-to-noise ratio. Optimal choice of EVFM domain will then involve eliminating such regions from the computations. This analysis will be pursued elsewhere.

Removal of the uniformity constraint on the VF also makes EVFM more versatile in handling missing data or regions with discontinuities. In fact, even the requirement of the domain being rectangular may be relaxed now, since any non-rectangular domain within the grid may be decomposed into constituent rectangular domains, the individual VW contributions of which may be added together to yield the VW equation for the entire domain. With these improvements, it is much easier to find appropriate EVFM domains when the measurement grid has missing data or is discontinuous.

5. Conclusions

1. In a typical experiment, since only the the total force is known, but not the actual distributions of tractions on the exterior surface, virtual displacement fields are usually required to be uniform over the regions on which tractions are applied so that the external virtual work can be easily computed in implementations of Virtual Fields methods. However, we show that although the traction at every point is not known,

it can still be written in terms of the unknown material parameters, thus leading to homogeneous equations. Thus, the requirement of uniformity of virtual fields is shown to be an unnecessary constraint.

2. Removal of the uniformity constraint is shown to lead to a more robust system of EVFM equations. The CVs of the computed parameters is shown to be much smaller than those reported in Nayakanti and Subramanian (2013).
3. The CVs of the computed parameters compare favourably with those obtained using conventional VFM.
4. Removal of the uniformity constraint enables arbitrary regions of the measurement grid to be used in EVFM. Internal regions can be used to generate ratios of the material parameters. In order to obtain unique values of the material parameters, the traction distribution or force resultant applied over a boundary area must be known and used in a VW equation.
5. With the uniformity constraint on VF removed, EVFM is now capable of handling material inhomogeneity, missing data and regions with discontinuities with ease.
6. The removal of the uniformity constraint also opens up the possibility of finding the domain that gives the best estimates of material properties for any given full-field strain data.

References

Grama, S. N., Subramanian, S. J., 2013. Computation of Full-Field Strains using Principal Component Analysis. Experimental Mechanics, Accepted

for Publication.

Grediac, M., 1989. Principe des travaux virtuels et identification/principle of virtual work and identification. Comptes Rendus de l'Academie des Sciences 309-II, 1–5.

Grediac, M., Toussaint, E., Pierron, F., 2002. Special Virtual Fields for the direct determination of material parameters with the Virtual Fields Method. 1 - Principle and definition. Int. J. Sol. Struct. 39, 2691–2705.

Malvern, L. E., 1977. Introduction to the Mechanics of a Continuous Medium. Prentice-Hall.

Nayakanti, N., Subramanian, S. J., 2013. Identification of Orthotropic Elastic Constants Using the Eigenfunction Virtual Fields Method. International Journal of Solids and Structures, Accepted for Publication.

Pierron, F., Grediac, M., 2012. The Virtual Fields Method: Extracting Constitutive Mechanical Parameters from Full-field Deformation Measurements. Springer.

Strang, G., 2006. Linear Algebra and its Applications. Cengage Learning.

Subramanian, S. J., 2013. The Eigenfunction Virtual Fields Method. Presented at the SEM Annual Congress and Exposition, Lombard, IL, USA.

Appendix A. Derivation of EVFM equations for VF3 and VF4

The Principle of Virtual Work is written for the virtual field VF3 (after cancelling out h throughout) as

$$\int_0^{L_2} \left[(Q_{11}\varepsilon_1(L_1, X_2) + Q_{12}\varepsilon_2(L_1, X_2)) - (Q_{11}\varepsilon_1(0, X_2) + Q_{12}\varepsilon_2(0, X_2)) \right] P_m(X_2; \boldsymbol{l}_1) \mathrm{d}X_2 - \int_0^{L_1} \int_0^{L_2} (Q_{66}\varepsilon_6(X_1, X_2)) f_m(X_2; \boldsymbol{l}_1) \mathrm{d}X_2 \mathrm{d}X_1 = 0 \quad \text{(A.1)}$$

The internal virtual work, the last term above, is evaluated by integrating along X_2 first and then over X_1. With the assumption of uniform strains over each element of the grid, the integration along X_1 becomes a summation of the X_2 integrals over the n values of X_1. Then, this term may be written as

$$\int_0^{L_1} \int_0^{L_2} (Q_{66}\varepsilon_6(X_1, X_2)) f_m(X_2; \boldsymbol{l}_1) \mathrm{d}X_2 \mathrm{d}X_1 = Q_{66}\Delta X_1 \sum_{k=1}^{n} \left[\int_0^{L_2} \varepsilon_6(X_1^k, X_2) f_m(X_2; \boldsymbol{l}_1) \mathrm{d}X_2 \right] \quad \text{(A.2)}$$

If the measured strain ε_6 is expanded in terms of the left eigenfunctions (Eqn. 8), the above expression becomes

$$Q_{66}\Delta X_1 \sum_{k=1}^{n} \left[\int_0^{L_2} \sum_{l=1}^{p} (\widetilde{\mathbf{A}}_6^c)^{(l,k)} f_m(X_2; \boldsymbol{l}_1) f_m(X_2; \boldsymbol{l}_1) \mathrm{d}X_2 \right], \quad \text{(A.3)}$$

which simplifies to

$$Q_{66}\Delta X_1 \Delta X_2 \sum_{k=1}^{n} (\widetilde{\mathbf{A}}_6^c)^{(1,k)} \quad \text{(A.4)}$$

due to the orthogonality of the eigenfunctions (Eqn. 6).

The first term of Eqn. (A.1) can be computed by direct integration. At any X_2, the virtual displacement field $u_2^* = P_m(X_2; \boldsymbol{l}_1)$ is computed by numerical integration of the function $f_m(X_2; \boldsymbol{l}_1)$:

$$P_m(X_2; \boldsymbol{l}_1) = \left[\sum_{k=1}^{j-1} l_1^k\right] \Delta X_2 + l_1^j (X_2 - X_2^j), X_2^j < X_2 < X_2^{j+1} \tag{A.5}$$

Then,

$$\begin{aligned} & Q_{11} \int_0^{L_2} \left[\varepsilon_1(L_1, X_2) - \varepsilon_1(0, X_2)\right] P_m(X_2; \boldsymbol{l}_1) \mathrm{d}X_2 \\ & = Q_{11} \sum_{j=1}^{m} \int_{X_2^j}^{X_2^{j+1}} \left(\varepsilon_1^{(n,j)} - \varepsilon_1^{(1,j)}\right) \left\{ \left[\sum_{k=1}^{j-1} l_1^k\right] \Delta X_2 + l_1^j \left(X_2 - X_2^j\right) \right\} \mathrm{d}X_2 \\ & = Q_{11} \sum_{j=1}^{m} \left(\varepsilon_1^{(n,j)} - \varepsilon_1^{(1,j)}\right) \left\{ \left[\sum_{k=1}^{j-1} l_1^k\right] (\Delta X_2)^2 + \frac{l_1^j}{2} \left((X_2^{j+1})^2 - (X_2^j)^2\right) - l_1^j X_2^j \Delta X_2 \right\} \end{aligned} \tag{A.6}$$

Similarly,

$$\begin{aligned} & Q_{12} \int_0^{L_2} \left[\varepsilon_2(L_1, X_2) - \varepsilon_2(0, X_2)\right] P_m(X_2; \boldsymbol{l}_1) \mathrm{d}X_2 \\ & = Q_{12} \sum_{j=1}^{m} \left(\varepsilon_2^{(n,j)} - \varepsilon_2^{(1,j)}\right) \left\{ \left[\sum_{k=1}^{j-1} l_1^k\right] (\Delta X_2)^2 + \frac{l_1^j}{2} \left((X_2^{j+1})^2 - (X_2^j)^2\right) - l_1^j X_2^j \Delta X_2 \right\} \end{aligned} \tag{A.7}$$

Substituting the expressions in Eqs. (A.4), (A.6) and (A.7) into Eqn. (A.1), we arrive at the expressions for P_{31}, P_{33} and P_{34} listed in Eqn. (16). A similar procedure applied to VF4 leads to the remaining expressions for P_{42}, P_{43} and P_{44}.